Machine Learning-based Regularization for Magnetic Particle Imaging

Corinna E. Rentschler

Darmstadt University of Applied Sciences - Faculties of Mathematics and Natural Sciences & Computer Science

Motivation

Magnetic Particle Imaging (MPI) is an emerging imaging modality which exploits the nonlinear magnetization of Superparamagnetic Iron Oxide (Nanoparticles) (SPIO) (cf. Fig. 1, left) in order to reconstruct the particle distribution in a scanned volume. The volume is sampled by the superposition of static and dynamic fields, adding up to a moving Field Free Point (FFP). The goal is to recover the spatial distribution of SPIO from a time dependent voltage signal that is measured by MPI.

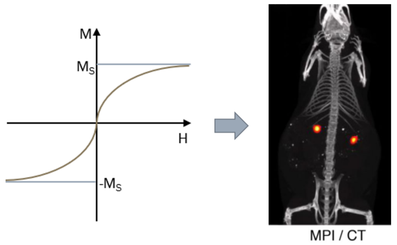

Figure 1. The nonlinear magnetization curve (left) is exploited to display the concentration distribution of injected SPIO tracers. The MPI signal is visualized in colors (right, Source: [Ta20]), whereas the structural information in grayscale is added by a CT scan.

Having been introduced by Gleich and Weizenecker [GW05] in 2005, MPI has been further developed as it promises high potential in medical imaging: It offers high spatial resolution, high temporal resolution and sensitivity [Wu+19]. Furthermore, neither X-Ray like in Computer Tomography (CT) nor radioactive tracers as in Positron Emission Tomography (PET) are used which offers an advantage for patients [Wu+19]. Comparable to PET images, MPI visualizes the concentration of tracers added to the scanned object (cf. Fig. 1, right).

Possible clinical applications:

- flow analysis eg. stenosis detection
- diagnostics of cancer cells [Häg+12]

MPI suffers from ill-posedness [KJL18], which leads to the need of regularization techniques in order to receive a stable solution. The fact that there are only few public accessible scan data challenges the usage of learning-based methods.

Goals of this work

The goal is to reconstruct the volume of SPIO concentration distribution from MPI data of a real MPI scanner. A standard Tikhonov regularization and two learning-based methods ought to be investigated, implemented and their results compared. Furthermore, the influence of different preprocessing steps should be analyzed by standard image quality measures.

References

[GW05] B. Gleich and J. Weizenecker. "Tomographic imaging using the nonlinear response of magnetic particles." In: Nature 435.7046 (2005), pp. 1214–1217

[Häg+12] J. Hägele et al. "Eisenoxidnanopartikel für Magnetic Particle Imaging (MPI)." In: RöFo - Fortschritte auf dem Gebiet der Röntgenstrahlen und der bildgebenden Verfahren 184.S 01 (2012)

[KJL18] T. Kluth et al. "On the degree of ill-posedness of multi-dimensional magnetic particle imaging." In: Inverse Problems 34.9 (2018), p. 095006

[Kno+18] T. Knopp et al. "MDF: Magnetic Particle Imaging Data Format." In: ArXiv e-prints (Jan. 2018). arXiv: 1602 . 06072v6 [physics.med-ph]

[Kno+20] T. Knopp et al. "OpenMPIData: An initiative for freely accessible magnetic particle imaging data." In: Data in brief 28 (2020), p. 104971. doi: 10.1016/j.dib.2019.104971

[Ta20] N. Taleblooo et al.: Magnetic Particle Imaging: Current Applications in Biomedical Research. In: Journal of magnetic resonance imaging (2020): JMRI 51 (6), S. 1659-1668

[Wu+19] L. C. Wu et al. "A Review of Magnetic Particle Imaging and Perspectives on Neuroimaging." In: AJNR. American journal of neuroradiology 40.2 (2019), pp. 206–212

Methods

As a result of a time-consuming calibration process, the MPI problem can be described as a linear system of equations that has to be inverted. Here, the system matrix S consisting of the discretized system answer multiplied with the unknown concentration vector c on the left hand side, should equal the measured voltage (vector) u on the right hand side of the equation leading to the system of linear equations Sc = u. This problem can be expressed as an optimization problem:

$$\hat{c} = \underset{c}{argmin} \ \frac{1}{2}||Sc - u||_2^2$$

Implemented regularization techniques for the reconstruction of MPI data of a real MPI scanner:

- **Standard Tikhonov Regularization**, L2-Regularization
- **Deep Image Prior** (DIP), learning-based
- **Plug and Play Prior** (PnP), learning-based

The Image quality of the results is quantified by the standard image quality measures Structural Similarity Index Measure (SSIM) and Peak Signal to Noise Ratio (PSNR).

Data

Publicly accessible data of the Open MPI dataset [Kno+20] provided in the Magnetic Particle Imaging Data Format (MDF) [Kno+18] are used to investigate the application of different regularization techniques. The calibration data, which are the foundation of the System Matrix, are aquired in a 19x19x19 grid using a reference phantom ("Delta phantom") containing a 100mmol/l tracer concentration, yielding to a reconstructed volume of 19x19x19 with a 2mmx2mmx1mm voxel size.
The scanned phantoms are shown in Fig. 2. Both phantoms are filled with a solution of 50mmol/l tracer concentration.

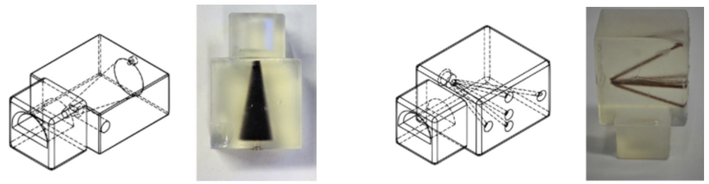

(a) Shape Phantom (b) Resolution Phantom

Figure 2. Phantoms used in the OpenMPIDatasets. Source: [Kno+20]

Acquired by a preclinical MPI scanner, the data inherit all properties of a real scan setup including noise and technology-induced perturbations. To tackle this challenge, the data are preprocessed with different preprocessing steps shown in Fig. 3.

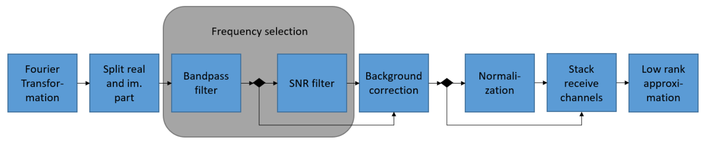

Figure 3. Preprocessing steps applied to MPI scan data.

Results

The different preprocessed MPI scan data are reconstructed by the three different regularization techniques and their corresponding hyperparameters are tuned. In Fig. 4, the center slices of some reconstructed volumes are shown.

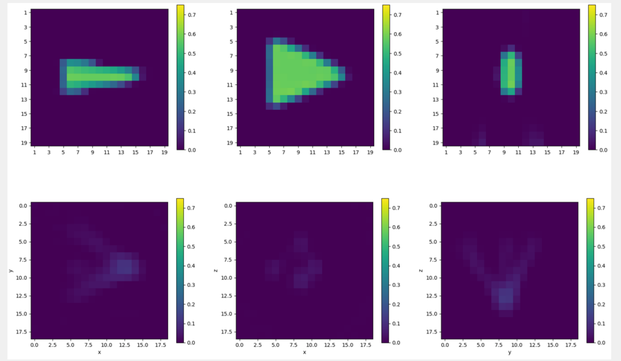

Figure 4. Middle slices of the reconstructions of the Shape phantom (top, PnP-reconstructed normalized data with signal to noise threshold 0) and the Resolution phantom (bottom, Tikhonov-reconstructed data, not normalized with signal to noise threshold 0).

The quantified evaluation of the reconstructed results is summarized in Fig. 5.

Shape Phantom	$PSNR_{max}$			$SSIM_{max}$		
Regularization Technique	$\tau = 0$	$\tau = 1$	$\tau = 5$	$\tau = 0$	$\tau = 1$	$\tau = 5$
Tikhonov Regularization	22.86	23.09	23.01	0.33	0.34	0.36
DIP	28.70	29.75	29.98	0.90	0.91	0.91
PnP	30.86	31.80	26.24	0.91	0.90	0.86

(a) Shape Phantom, normalized data

Shape Phantom	$PSNR_{max}$			$SSIM_{max}$		
Regularization Technique	$\tau = 0$	$\tau = 1$	$\tau = 5$	$\tau = 0$	$\tau = 1$	$\tau = 5$
Tikhonov Regularization	22.28	22.38	22.64	0.32	0.32	0.39
DIP	26.75	29.35	30.39	0.88	0.90	0.91
PnP	30.30	30.10	25.78	0.90	0.90	0.85

(b) Shape Phantom, not normalized data

Resolution Phantom	$PSNR_{max}$			$SSIM_{max}$		
Regularization Technique	$\tau = 0$	$\tau = 1$	$\tau = 5$	$\tau = 0$	$\tau = 1$	$\tau = 5$
Tikhonov Regularization	30.23	30.24	30.23	0.38	0.37	0.39
DIP	31.69	28.48	32.45	0.33	0.25	0.35
PnP	29.02	28.96	30.00	0.28	0.29	0.30

(c) Resolution Phantom, normalized data

Resolution Phantom	$PSNR_{max}$			$SSIM_{max}$		
Regularization Technique	$\tau = 0$	$\tau = 1$	$\tau = 5$	$\tau = 0$	$\tau = 1$	$\tau = 5$
Tikhonov Regularization	29.98	30.28	30.03	0.33	0.27	0.33
DIP	31.67	32.45	31.07	0.30	0.32	0.33
PnP	29.06	29.02	29.02	0.27	0.28	0.29

(d) Resolution Phantom, not normalized data

Figure 5. Best results of preprocessed MPI data and different applied regularization techniques. The highest achieved image quality values are underlined for each preprocessed data investigated.

Conclusion

The main findings of this work are:

- The Standard Tikhonov regularization provides comparably good results in the reconstruction of the Resolution phantom. The regularization parameter controls the tradeoff between lower frequent and higher frequent parts of the image.
- Reconstructions using DIP are highly dependent on the chosen hyperparameters. Early stopping is necessary.
- The hyperparametertuning of PnP is non-trivial and crucial for the resulting image quality. Different slicing methods are tested: A random choice of the slice axis provides better results.

corinna.e.rentschler@stud.h-da.de